

# In vitro investigation of flower-like micro-nano topography modifications to improve titanium implant surface properties

Investigação in vitro de modificações em formato de flor de micro-nano topografia para melhorar as propriedades da superfície de implantes de titânio

Nadia KARTIKASARI<sup>1</sup> , Ratri Maya SITALAKSMI<sup>1</sup> , Karina MUNDIRATRI , Salsabilla Eliya ANDARU<sup>1</sup> ,  
Aisyah Rachmadani Putri GOFUR<sup>1</sup> , Harry LAKSONO<sup>1</sup> 

1 - Universitas Airlangga, Faculty of Dental Medicine, Department of Prosthodontics, Surabaya, Jawa Timur, Indonesia.

**How to cite:** Kartikasari N, Sitalaksmi RM, Mundiratri K, Andaru SE, Gofur ARP, Laksono H. In vitro investigation of flower-like micro-nano topography modifications to improve titanium implant surface properties. *Braz Dent Sci.* 2025;28(1):e4663. <https://doi.org/10.4322/bds.2025.e4663>

## ABSTRACT

**Objective:** The surface modification of titanium implants has demonstrated significant potential in enhancing the surface characteristics of the implants, improving their performance, and minimizing the risk of infection. This study examines the advantages of combining acid etching and alkaline heat treatment to enhance titanium implant surfaces and evaluate their antibacterial effectiveness. **Material and Methods:** Titanium was divided into four groups: machine surface (MA), samples subjected to a single acid etching (MR), and samples that experienced both a single acid etching and two distinct alkaline heat treatment protocols (MN1 and MN2). The surface properties (topography, chemical composition, surface roughness, and wettability) and antibacterial evaluation against *Porphyromonas gingivalis* were evaluated. The statistical significance of differences among the groups was determined using ANOVA and Tukey's Post-Hoc Test ( $P < 0.05$ ). **Results:** The MN group significantly transformed titanium surfaces into a micro-nano flower-like topography with hydroxyl and sodium titanate structures. The highest surface roughness was shown in MN1 ( $S_a = 7,58 \pm 0,64$ ;  $S_q 9,78 \pm 0,8$ ) ( $P < 0.05$ ) and the lowest wettability were shown in MN2 ( $25,75 \pm 8,2$ ) ( $P < 0.05$ ). Conversely, MN2 exhibited the lowest wettability, measured at  $25.75 \pm 8.2$  ( $P < 0.05$ ). Antibacterial assessments revealed a notable reduction in the growth of *Porphyromonas gingivalis* on the MN2 modified surfaces at  $27.43 \pm 10.43\%$  ( $P < 0.05$ ). **Conclusion:** The combination of acid etching and alkaline heat treatment has shown the ability to create a micro-nano surface with outstanding properties and significant antibacterial effects. This advancing titanium dental implant technology presents a valuable alternative for improving clinical outcomes in dental applications.

## KEYWORDS

Antibacterial agents; Dental implant; Medicine; Surface properties; Titanium.

## RESUMO

**Objetivo:** A modificação da superfície dos implantes de titânio tem demonstrado potencial significativo na melhoria das características da superfície dos implantes, melhorando seu desempenho e minimizando o risco de infecção. Este estudo examina as vantagens da combinação de ataque ácido e tratamento térmico alcalino para melhorar as superfícies de implantes de titânio e avaliar sua eficácia antibacteriana. **Materiais e métodos:** O titânio foi dividido em quatro grupos: superfície de máquina (MA), amostras submetidas a um único ataque ácido (MR) e amostras submetidas a um único ataque ácido e dois protocolos distintos de tratamento térmico alcalino (MN1 e MN2). Foram avaliadas as propriedades da superfície (topografia, composição química, rugosidade e molhabilidade) e a avaliação antibacteriana contra *Porphyromonas gingivalis*. As diferenças estatísticas significantes entre os grupos foram determinadas por meio de ANOVA e teste post-hoc de Tukey ( $p < 0,05$ ). **Resultados:** O grupo MN transformou significativamente as superfícies de titânio em uma micro-nanotopografia em forma de

flor, com estruturas de hidroxila e titanato de sódio. A maior rugosidade superficial foi observada em MN1 ( $Sa = 7,58 \pm 0,64$ ;  $Sq = 9,78 \pm 0,8$ ) ( $P < 0,05$ ) e a menor molhabilidade foi observada em MN2 ( $25,75 \pm 8,2$ ) ( $P < 0,05$ ). Por outro lado, MN2 apresentou a menor molhabilidade medida em  $25,75 \pm 8,2$  ( $P < 0,05$ ). As avaliações antibacterianas revelaram uma redução notável no crescimento de *Porphyromonas gingivalis* nas superfícies modificadas com MN2 em  $27,43 \pm 10,43\%$  ( $P < 0,05$ ). **Conclusão:** A combinação de ataque ácido e tratamento térmico alcalino demonstrou a capacidade de criar uma micro-nano superfície com propriedades excepcionais e efeitos antibacterianos significativos. Esta tecnologia avançada de implantes dentários de titânio apresenta uma alternativa valiosa para melhorar os resultados clínicos em aplicações odontológicas.

## PALAVRAS-CHAVE

Agentes antibacterianos; Implante dentário; Medicina; Propriedades de superfície; Titânio.

## INTRODUCTION

Titanium implants are widely recognized as the gold standard in dental implantology due to their exceptional biomechanical and biocompatible properties [1-4]. However, the peri-implantitis poses a significant challenge in the application of titanium implants [1]. As titanium is classified as a bioinert material, it possesses no intrinsic antimicrobial properties. Consequently, this can facilitate bacterial colonization, which may obstruct the integration with adjacent tissues, prolong the postoperative recovery period, and compromise the overall health, aesthetics, and functionality of dental implant restorations [2].

One of the key factors contributing to peri-implantitis associated with titanium implants is the colonization of bacteria. Microorganisms such as *Prevotella intermedia*, *Fusobacterium nucleatum*, and *Porphyromonas gingivalis* play an essential role in its development and progression through biofilm formation [5]. Once the titanium surface is exposed to the oral environment, bacteria begin to adhere to the titanium surface and form a biofilm. These biofilms are characterized by complex three-dimensional structures composed of extracellular polymeric substances that effectively protect bacterial clusters, enabling their long-term persistence [6]. This protective layer shields bacteria from antibacterial agents, antibiotics, nutrient deprivation, and immune responses, making them more resistant to treatment [1]. The use of antibacterial agents can further exacerbate bacterial resistance, creating a significant challenge in effectively managing peri-implant infections.

Recent advancements in the surface modification of titanium implants at the micro-nanometer scale topography level have gained significant attention due to their ability to alter both

surface topography and chemical composition. The alteration of the surface topography, roughness, chemical composition, wettability, and electric charge, play a crucial role in bacterial adhesion and biofilm formation on implant surfaces [6-10]. Consequently, optimizing these parameters may improve the antibacterial efficacy of the implants [4]. Although these properties can be manipulated to mitigate biofilm formation, it remains challenging to control external environmental factors such as pH, temperature, bacterial species, morphology, and size [7].

The effectiveness of bactericidal surfaces is influenced by several factors, including topography, structural height, radius, and spacing. Surfaces designed to prevent bacterial adhesion can be categorized as either bactericidal or anti-biofouling. Bactericidal surfaces compromise the integrity of the bacterial cell wall, ultimately resulting in cell death. In contrast, anti-biofouling surfaces inhibit and deter bacterial attachment through specific topographical or chemical properties [1]. Micro-topographies typically possess antifouling characteristics by inhibiting bacterial adhesion, whereas nano-topographies demonstrate antibacterial capabilities by directly rupturing bacterial membranes and resulting in cell death [11,12]. Implant surface modification significantly enhances the contact adhesion area, thereby improving the bactericidal properties of surfaces compared to the smooth or no treatment surface [13]. This micro-nano topography leads to mechanical damage on bacterial membranes through direct contact, generating physical stress that contributes to enhanced bactericidal effects [1].

Acid etching represents a surface modification technique wherein titanium implants are immersed in strong acidic solutions, including hydrochloric acid (HCl), nitric acid (HNO<sub>3</sub>), sulfuric acid (H<sub>2</sub>SO<sub>4</sub>), or hydrofluoric acid (HF), under controlled conditions [2,8]. This procedure

yields a micro-rough topography characterized by uniformly distributed ridges and pits [13-20]. Although these micron-scale topographies do not possess inherent bactericidal properties, they influence the interactions between bacteria and surfaces, thereby reducing bacterial adhesion and obstructing biofilm formation [8]. Conversely, alkali-heat treatment is a method in which titanium is immersed in strong alkaline solutions, such as sodium hydroxide (NaOH) or potassium hydroxide (KOH), followed by exposure to elevated temperatures in a furnace for a specified duration [2,8,13-16]. This treatment facilitates the development of titanium oxide nanospikes, which exhibit bactericidal potential through the mechanical disruption of bacterial cell membranes [21]. Furthermore, titanium nano surfaces characterized by dense, anisotropically patterned nano spikes demonstrate antimicrobial activity by repelling Gram-positive cocci and effectively eliminating Gram-negative bacilli [18].

Implant surface modifications were used to achieve micro- and nano-scale topography in order to increase biological efficacy. Prior research indicates that nano-scale topographies can address the limitations associated with micro-scale structures by facilitating cell spreading and significantly promoting osteoblast differentiation and osseointegration [22]. In addition, micro-nano hierarchical surfaces promote improved osteoblast adhesion and proliferation by closely resembling the topography natural bone [23]. Micro-nano hierarchical surfaces significantly enhance the adhesion and proliferation of osteoblasts by effectively mimicking the topographical characteristics of natural bone [24]. Their results indicated that the incorporation of nano-topography to micro-topography led to enhanced cell proliferation while preserving mechanical interlocking and promoting differentiation [2]. In light of these results, we would like to integrate the micro topography produced by acid etching and the alkaline heat treatment's nano topography. This study aims to assess the efficacy of the combined application of acid etching and alkali-heat treatment in terms of its surface properties (topography, chemical composition, surface roughness, and wettability) and antibacterial effectiveness. Our hypothesis is that the combination of acid etching and alkaline heat treatment may induce suitable titanium surface properties and enhance antibacterial effectiveness.

## MATERIALS AND METHODS

This laboratory experiment was an in vitro study employing a post-test-only control group design. Ethical approval for the research was obtained from the Health Research Ethical Clearance Committee of the Faculty of Dental Medicine at Universitas Airlangga (No. 0870/HRECC.FODM/VIII/2024). The study focused on examining the topography, surface roughness, and chemical composition that define the surface characteristics at the Department of Materials and Metallurgical Engineering, Institute of Technology Sepuluh Nopember (ITS). Additionally, the wettability and antimicrobial activity of the materials were assessed against *Porphyromonas gingivalis* at the Research Center of the Faculty of Dental Medicine, Universitas Airlangga (Figure 1). Each sample were evaluated triplicate and the number of samples of each group is three.

### Preparation of titanium surface

This study employed commercially pure-grade I titanium plates, which were purchased from PT Special Metals, Jakarta, Indonesia. The titanium plates were subjected to laser cutting to create square-shaped samples measuring 10 mm x 10 mm x 5 mm. Titanium were divided into four main group: machine surface (MA), Ti samples underwent a single acid etching (MR), Ti sample underwent single acid etched and two alkaline heat treatment protocols (MN1 and MN2). The machine titanium (MA) underwent a thorough cleansing process utilizing a series of ethanol and distilled water, followed by ultrasonication.

The acid-etched surfaces were prepared by immersed the MA titanium samples in a 67% (w/w) sulfuric acid solution (Merck, Darmstadt, Germany) at a temperature of 120°C for a duration of 75 seconds. Upon completion of the etching procedure, the titanium surfaces were allowed to dry at room temperature and were subsequently designated as micro-roughened (MR) surfaces.

The combination of acid etching and alkaline heat treatment were expected to produce micro-nano roughened (MN). Two distinct alkaline heat treatments were administered to the MR samples, according to the previous protocol [13-16]. In summary, the MR samples were boiled in a sodium hydroxide (NaOH) solution (Merck, Darmstadt, Germany) for a period of 24 hours. The alkaline

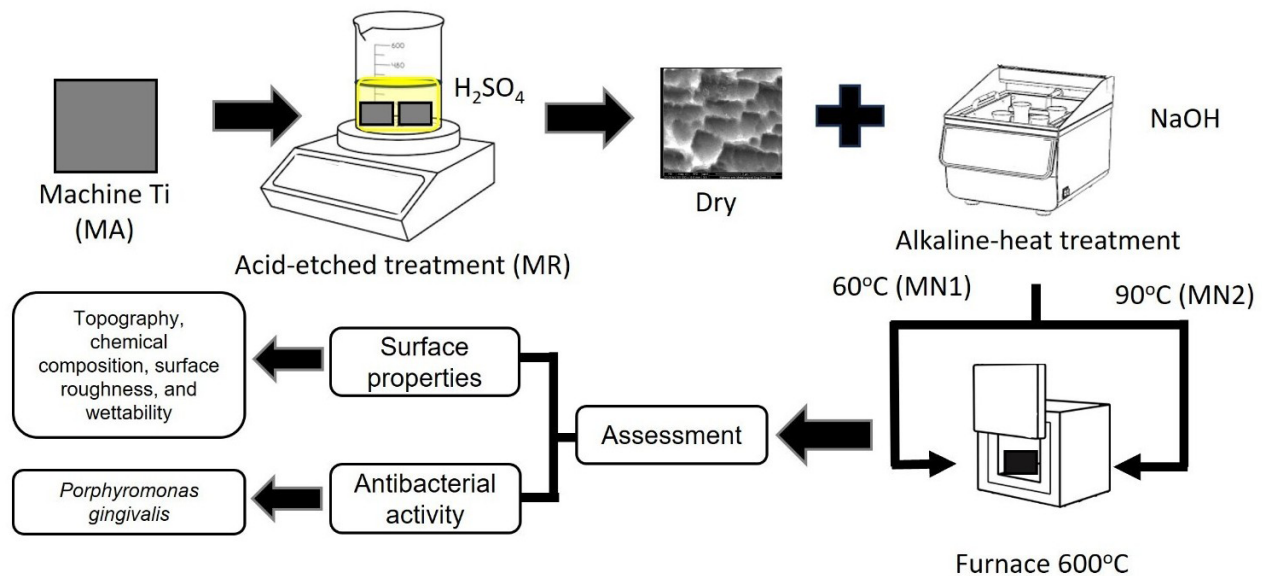


**Figure 1** - Research Diagram. Machine titanium grade 1 (MA) was prepared (10 mm x 10 mm x 5 mm). The treated titanium group was Ti samples that underwent a single acid etching (MR), Ti samples underwent single acid etching and two alkaline heat treatment protocols (MN1 and MN2). For the acid etched treatment, MA titanium samples were placed in a 67% (w/w) sulfuric acid solution at a temperature of 120°C for 75 seconds. Alkaline heat treatment was conducted using 5M sodium hydroxide solution at 60°C, designated as micro-nano roughened surface 1 (MN1), while the second treatment involved a 10M solution at 90°C, designated as micro-nano roughened surface 2 (MN2). The surface properties and antibacterial effect were evaluated after the Ti sample preparation.

heat treatments were categorized as follows: the first treatment utilized a 5M sodium hydroxide solution at 60°C, designated as micro-nano roughened surface 1 (MN1), while the second treatment involved a 10M solution at 90°C, designated as micro-nano roughened surface 2 (MN2). Following the boiling process, the titanium samples underwent rinsing with distilled water, were air-dried overnight, and then subjected to sintering in a furnace at 600°C for one hour before being allowed to cool to ambient temperature.

### Scanning Electron Microscope-Energy Dispersive X-Ray (SEM-EDX)

The topography of the titanium samples was assessed utilizing scanning electron microscopy (SEM) with an FEI Inspect-S50 system (Oregon, USA). The SEM images of the titanium samples were taken at magnifications of 10000x, 15000x, and 50000x to enable a comprehensive examination of the surface morphology. Furthermore, elemental analysis of the titanium surfaces was carried out using energy-dispersive X-ray spectroscopy (EDX), which is incorporated into the SEM system.

### Fourier transform infrared (FTIR) spectroscopy

Functional groups on the titanium surface were analyzed using Fourier transform infrared

(FTIR) spectroscopy Thermo Scientific Nicolet iS10 (Wisconsin, USA). The spectra were recorded in the range of 4000–2000 cm<sup>-1</sup>. Background correction was performed based on the surface spectrum of MA.

### X-ray diffraction (XRD)

The crystalline phase of each titanium surface was analyzed using MiniFlex 600C X-ray diffractometer (Tokyo, Japan). Titanium discs were analyzed with Cu K $\alpha$  radiation ( $\lambda = 1.5406 \text{ \AA}$ , 40 kV, 40 mA). Diffraction patterns were collected in the  $2\theta$  range of 10° to 90°

### Atomic Force Microscopy (AFM)

The surface roughness of the titanium samples was assessed using an Atomic Force Microscopy (AFM) device (Bruker-Nano N8 NEOS, Bruker Corp., Billerica, MA, USA). The surface roughness parameters that were measured included the arithmetical mean height ( $S_a$ ), root mean squared height ( $S_q$ ), maximum height ( $S_z$ ), and maximum surface amplitude ( $S_t$ ).

### Wettability

The wettability of the titanium surface was assessed by single-drop of 10  $\mu\text{L}$  of distilled water onto the titanium surface. The images of the contact angle were obtained using a camera

(Fujifilm, Tokyo, Japan). The contact angle measurements were subsequently analyzed and calculated using ImageJ 1.54g software developed by National Institutes of Health and the Laboratory for Optical and Computational Instrumentation (LOCI, University of Wisconsin), USA).

### *Porphyromonas gingivalis* culture

*Porphyromonas gingivalis* (ATCC 33277, United Kingdom) was obtained from the culture stock. The bacteria were first grown in Tryptone Soya Broth (TSB) and incubated anaerobically at 37°C for 18–24 hours. Bacterial colonies were then collected using a sterile loop and transferred to 3 mL of Brain Heart Infusion (BHI) liquid media, followed by incubation at 37°C for 18 hours. The bacterial suspension was standardized to match a McFarland standard of 0.5 ( $1.5 \times 10^8$  CFU/mL). The standardized suspension was carefully pipetted and evenly spread onto the surface of nutrient agar media.

### Antibacterial activity

Titanium samples were incubated in centrifuge tubes containing 5 mL of *Porphyromonas gingivalis* suspension for 24 hours. Following the incubation, the tubes were vortexed to dislodge adherent bacteria from the titanium surface. Subsequently, 0.1 mL of the resulting suspension was plated onto Mueller Hinton Agar (MHA) medium in petri dishes and incubated at 37°C for 48 hours under anaerobic conditions. After the incubation period, bacterial colonies were enumerated to determine the bacterial load. The bactericidal ratio was calculated using the following formula:

$$BR\% = \frac{CFUs_{(1)} - CFUs_{(2)}}{CFUs_{(1)}} \cdot 100 \quad (1)$$

Where  $CFU_{(1)}$  represents the colony-forming units in the control group, and  $CFU_{(2)}$  represents the colony-forming units in the experimental group.

After completing the data collection, a statistical analysis was conducted using SPSS software 27 (IBM, Tokyo, Japan). The normality of the data was assessed using the Kolmogorov-Smirnov test ( $P > 0.05$ ), and homogeneity was evaluated using Levene's test ( $P > 0.05$ ). When appropriate, One-Way ANOVA ( $P < 0.05$ ) was used to assess significant differences among the groups. Following this, the Post Hoc Tukey's

Honestly Significant Difference (HSD) test ( $P < 0.05$ ) was performed to enable specific comparisons between the groups.

## RESULTS

The surface treatment applied to the titanium modified its appearance, changing from the original silver metallic hue to a dark grey following acid etching. Conversely, the combination of acid and alkaline heat treatments resulted in a light brown-yellowish tint for the group combination acid etching and alkaline heat treatment with 5M NaOH (MN1) and a dark brown color for the group combination acid etching and alkaline heat treatment with 10M NaOH (MN2) (Figure 2A). The scanning electron microscopy (SEM) images of the machine titanium treatment (MA) group revealed a flat surface characterized by a broad groove (Figure 2B a-a'-a'"). In contrast, the group with acid etching treatment (MR) exhibited titanium surfaces displaying a relatively uniform distribution of numerous sharp ridges and pits, which formed outer honeycomb-like grooves of varying sizes (Figure 2B b-b'-b'"). Both MN1 and MN2 exhibited a nanoflower-like structure, however, MN1 displayed additional filopodia-like petal extensions radiating outward (Figure 2B c-c'-c'"), while MN2 presented a more compact nanoflower characterized by thicker petal-like formations that were tightly clustered around the center, featuring overlapping layers (Figure 2B d-d'-d'"). Elemental analysis indicated that both the machine titanium (MA), titanium with acid etching (MR), and MN1 groups were composed of titanium (Ti) and oxygen (O), whereas MN2 contained titanium, oxygen, and sodium (Na). In all groups, titanium was the predominant component (Figure 2C).

### The FTIR spectra analysis of titanium samples interpreted the chemical composition.

The MN1 and MN2 groups demonstrated distinct hydroxyl (O-H) stretching peaks within the 3700–3590  $\text{cm}^{-1}$  range [25]. Specifically, MN1 exhibited a peak at 3629.1  $\text{cm}^{-1}$ , whereas MN2 displayed a peak at 3638.1  $\text{cm}^{-1}$  (Figure 3A, lower panel). X-ray diffraction (XRD) patterns, which serve as an indication of the chemical composition of the samples, confirmed that the MA group did not include titanium dioxide ( $\text{TiO}_2$ ) and sodium titanate. Similarly, the MR group displayed no detectable peaks associated with the

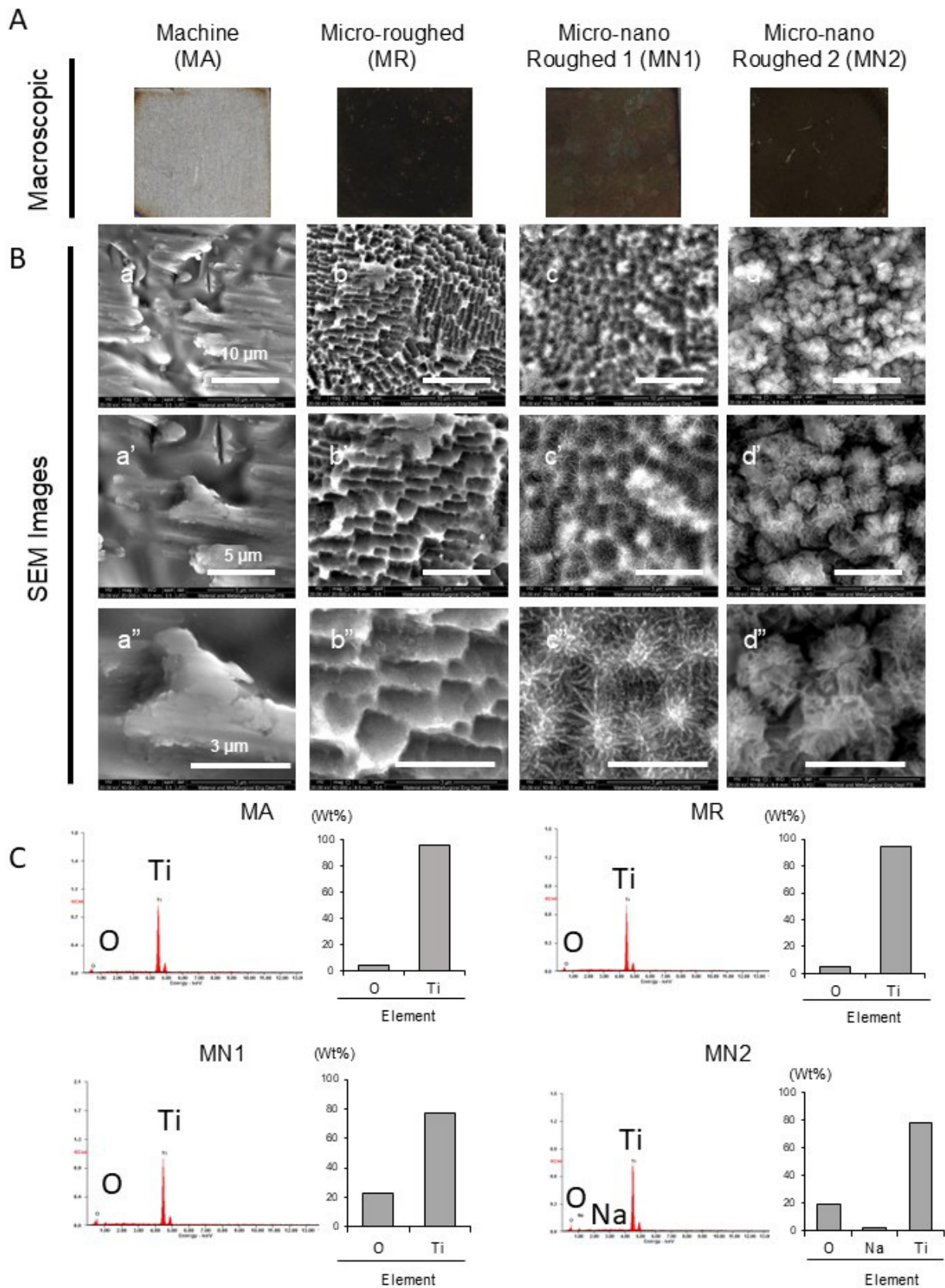


**Figure 2** - Surface topography of the titanium surfaces. (A) Representative of the macroscopic features of the machine (MA), micro-roughed (MR), micro-nano roughed 1 (MN1) and micro-nano roughed 2 (MN2) surfaces. (B) Representative scanning electron microscope (SEM) images in each titanium surfaces at magnification 10.000x (a,b,c,d), 20.000x (a',b',c',d'), and 50.000x (a'', b'',c'',d'') (C) Representative of Energy Dispersive X-Ray in each titanium surfaces (N=3).

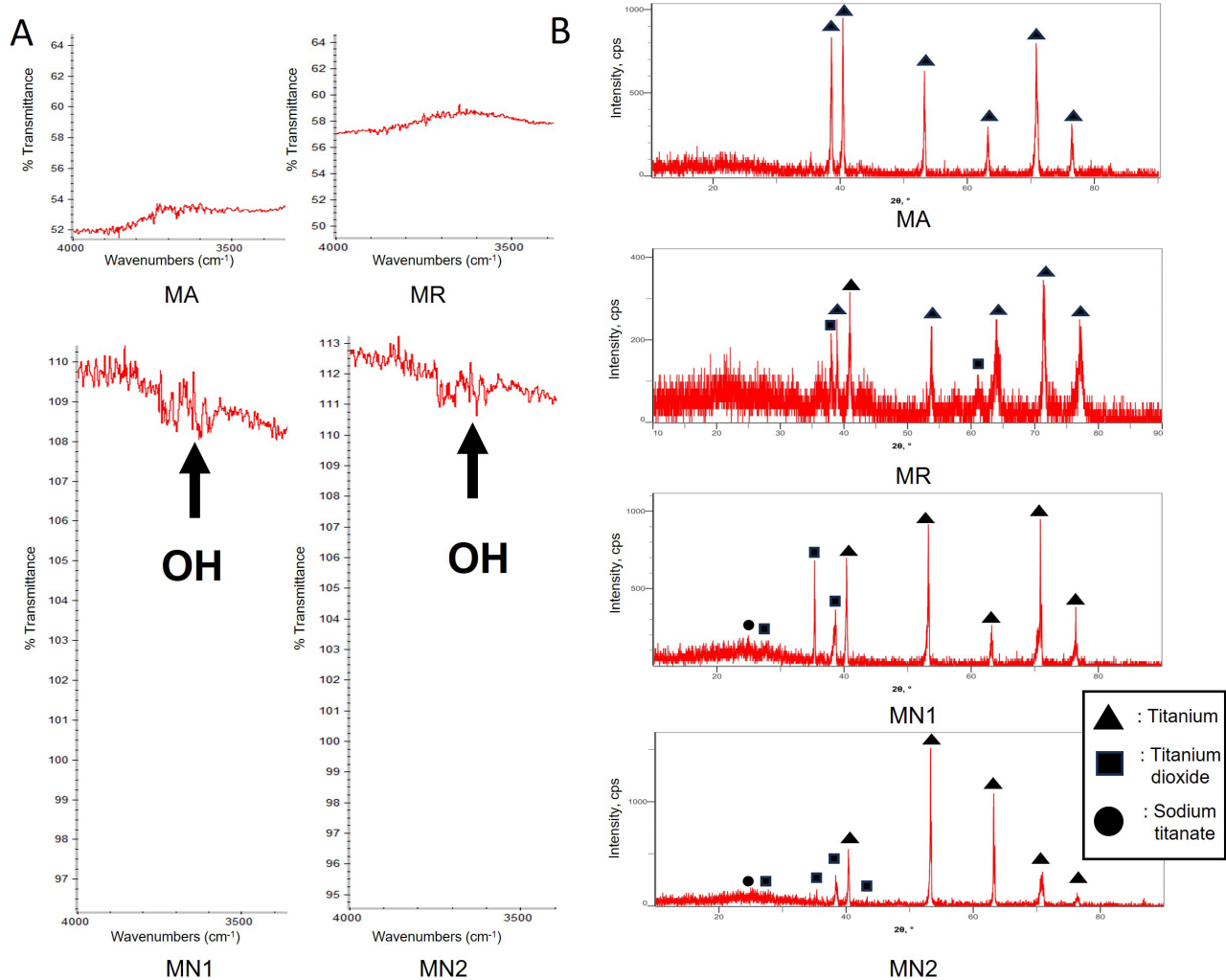


**Figure 3** - Chemical composition of the titanium surfaces. (A) Fourier transform infrared (FTIR) spectra of the machine (MA), micro-roughed (MR), micro-nano roughed 1 (MN1) and micro-nano roughed 2 (MN2) surfaces. (B) X-ray diffraction (XRD) features in each titanium surfaces. (N=3).

phases of sodium titanate. This lack of detectable peaks indicates that these compounds were absent from the surfaces of the MA and MR groups. The findings suggest that the surface treatments applied to the MN samples effectively facilitated the formation of rutile crystallite TiO<sub>2</sub> structure and sodium titanate, a process that did not occur in the MA and MR groups (Figure 3B). Titanium dioxide (TiO<sub>2</sub>) has been recognized for its potential antibacterial properties [26,27], while sodium titanate, an inorganic ion exchanger, has also been reported to exhibit both antibacterial and antifungal activities [28].

Following the modification of titanium surfaces, all experimental groups exhibited an increase in surface roughness. The parameters Sa and Sq indicated that the MN1 group demonstrated the highest roughness values, with Sa and Sq measurements being 2.20 and 2.00

times greater, respectively, than those of the MA group. Nevertheless, the roughness values for the MN1 group were comparable to those observed in the MR group. MN2 showed a similar surface roughness with MR. No significant differences were detected in the Sz and St values across the groups (Figure 4A). Water contact angles were measured to assess hydrophilicity, serving as an indicator of surface wettability. Contact angles exceeding 90° are classified as hydrophobic, those below 90° as hydrophilic, and measurements falling beneath 10° as superhydrophilic [13]. In this investigation, all groups exhibited hydrophilic characteristics, with the MN1 and MN2 groups displaying significantly lower contact angles in comparison to the other groups (Figure 4B).

Antibacterial activity against *Porphyromonas gingivalis* was assessed by monitoring the development of colonies characterized by a

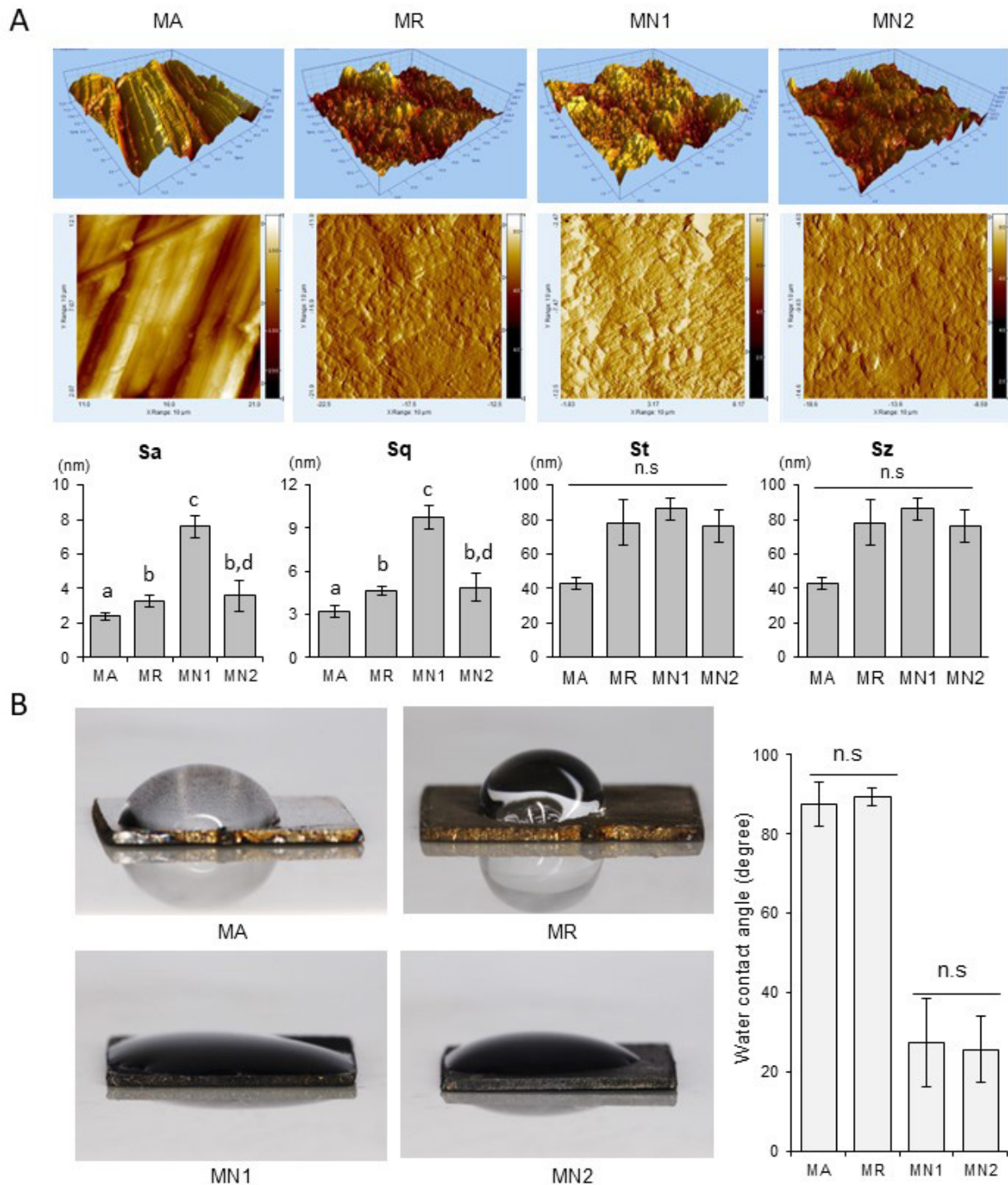


**Figure 4** - Surface roughness and wettability of titanium surfaces. (A) Surface roughness of the machine (MA), micro-roughed (MR), micro-nano roughed 1 (MN1) and micro-nano roughed 2 (MN2) surfaces from Atomic Force Microscopy (AFM) analysis (first and second row). Vertical roughness parameter Sa, Sq, St, and Sz (third row). (B) Water contact angle of the titanium surfaces. Data presented as means  $\pm$  standard deviation (SD) (N = 3). Different letters or asterisks indicate statistically significant differences between them ( $P < 0.05$ ; Tukey's honestly significant difference [HSD] test. arithmetic mean height (Sa), root mean squared height (Sq), maximum height (Sz), and maximum surface amplitude (St).

yellowish-white coloration (Figure 5A). The MN group exhibited a statistically significant difference compared to the MA and MR1 groups, however, no significant difference was observed between the MN1 and MN2 groups (Figure 5B).

The highest bacterial ratio, utilized to evaluate the percentage of bacterial death, was recorded in the MN2 group. Furthermore, no significant disparities were found between the MR and MN1 groups (Figure 5B).

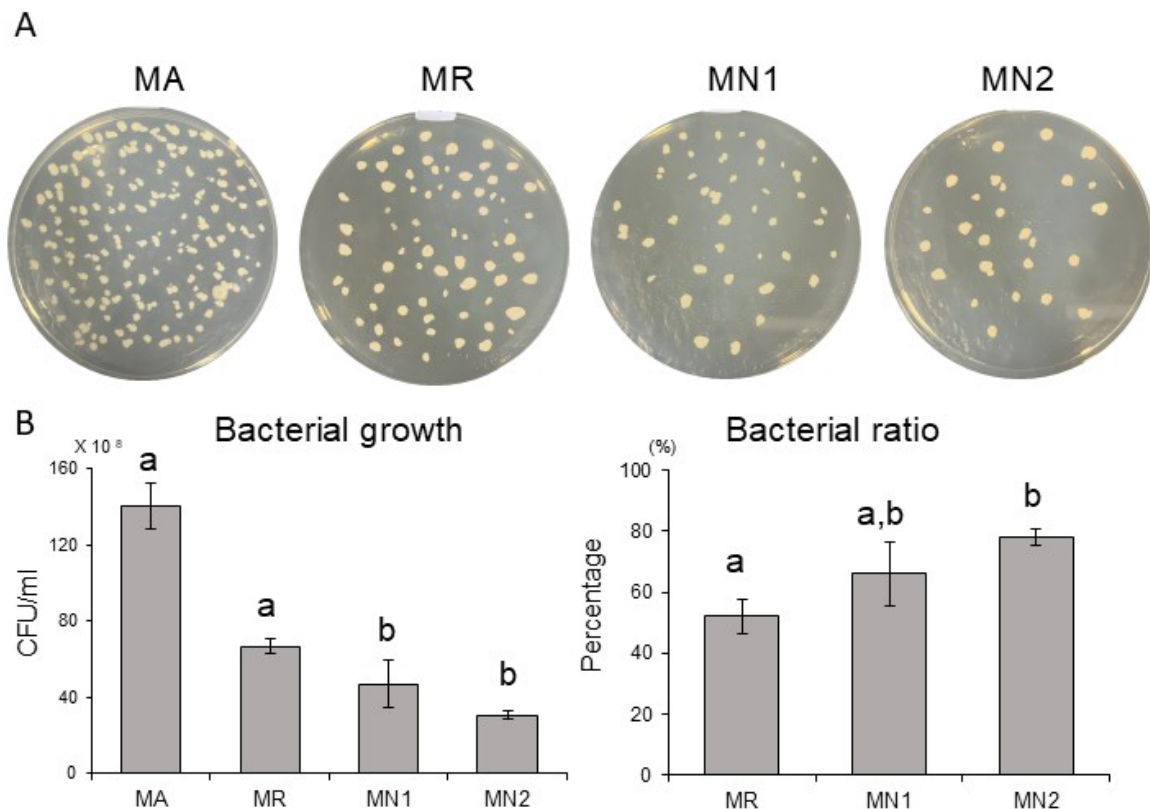


**Figure 5** - (A) Antibacterial activity against *Porphyromonas gingivalis*. Representative of the macroscopic features of bacterial growth in the machine (MA), micro-roughed (MR), micro-nano roughed 1 (MN1) and micro-nano roughed 2 (MN2) surfaces. (B) The quantification of the bacterial growth and bacterial ratio. Data presented as means  $\pm$  standard deviation (SD) (N = 3). Different letters or asterisks indicate statistically significant differences between them ( $P < 0.05$ ; Tukey's honestly significant difference [HSD] test).

## DISCUSSION

Surface modification is critical for enhancing the topography and composition of implant surfaces. The primary objectives of these modifications are to decrease wettability, and increase surface roughness and antibacterial properties, thereby facilitate osteoblast attachment and ensure effective osseointegration [29]. The most widely method for combination of surface modification is acid etching. Additionally, alkali-heat treatment may be implemented to further refine surface characteristics. In this study, a combination of micro-scale surface modification through acid etching and alkali-heat treatment was employed to generate a nano-structured surface, resulting in a surface that integrates both micro and nano-scale features. In comparison with single micro or nano topography, hierarchical micro-nano topography has a great deal of potential to promote osteogenesis because it has a combination of benefits. The nano-scale structure could increase protein adsorption, cell adhesion,

and ultimately osseointegration, while the micro-scale structure may strengthen the interlocking of the bone with the implant [22].

The acid-etched treatment produced uniform, distinct ridges, and pits, resulting in a honeycomb-like surface texture characterized by grooves of varying sizes similar to prior studies [13,15,20,30]. The previous research indicated that alkaline-heat treatment generated dense nanosized spikes. Notably, alkaline heat with 5M NaOH displayed a relatively isotropic distribution of nanospikes, whereas alkaline heat with 10M NaOH exhibited an anisotropic distribution [13-16]. The integration of acid etching and alkaline-heat treatment yielded a flower-like structure with distinct morphological features. Combination of acid etched and alkaline heat with 5M NaOH (MN1) presented filopodia-like petal extensions radiating outward, while combination of acid etched and alkaline heat with 10M NaOH (MN2) showed a more compact configuration with thicker, densely clustered petal-like formations, accompanied by overlapping

layers. This flower-like topography, representing a micro-nano structure, demonstrated significant antibacterial properties by imposing physical stress on bacterial surfaces. The unique architectural design produced shearing forces during bacterial adhesion, resulting in substantial membrane stress that mechanically disrupted bacterial membranes, thereby enhancing physical sterilization efficacy [1].

Hydroxyl structures have been identified in the MN groups, a characteristic typically associated with alkaline heat treatment. Hydroxyl groups are recognized for their robust oxidative properties, which contribute to the generation of reactive oxygen species (ROS). These ROS are significant contributors to bacterial cell toxicity due to the induction of oxidative stress [24]. Chemical analysis of the MN group has revealed the presence of  $\text{TiO}_2$  and sodium titanate.  $\text{TiO}_2$  is a material known for its diverse physical and chemical properties, and it is widely acknowledged for its strong antibacterial and antifungal activities against both Gram-positive and Gram-negative bacteria. This study identified the rutile crystallite phase of  $\text{TiO}_2$  within the MN group, a phase known for its stability and exceptional antibacterial efficacy [25-27]. Furthermore, sodium titanate was also detected in the MN group. Previous reports indicate that sodium titanate enhances surface hydrophilicity by reducing wettability. Surfaces that exhibit high hydrophilicity particularly have a high antibacterial activity [28,31]. The analysis of the chemical composition was in line with the findings of the elemental study, which identified Ti, O, and Na only within the MN2 group, therefore, the presence of  $\text{TiO}_2$  and sodium titanate was confirmed to be specific to this group.

Surface roughness and wettability are essential factors that significantly affect bacterial adhesion. Extensive research indicates that bacteria prefer adhering to rough surfaces rather than smooth ones, with a marked inclination toward hydrophilic surfaces over hydrophobic ones [2,7,32]. Although an increase in surface roughness typically correlates with an enlarged surface area and a higher potential for bacterial adherence, under specific conditions it may conversely contribute to a reduction in bacterial colonization. Previous report also shown that micro-nano topographic surfaces have demonstrated significant mechano-bactericidal activity, thereby challenging the conventional

paradigm [33,34]. In this study, the application of surface treatments resulted in a substantial increase in roughness compared to the MA group. The MN surfaces demonstrated a higher level of roughness than the MR surfaces. Within the MN group, MN1 exhibited the greatest roughness, followed by MN2. Acid-etched surfaces typically displayed hydrophobic properties, whereas superhydrophilic properties characterized surfaces subjected to alkaline-heat treatment [13-16]. Notably, the combination of acid-etching and alkaline-heat treatment produced surfaces that were more hydrophilic than those that were solely acid-etched, although they did not attain superhydrophilic characteristics. This is a similar result with previous study also shown the micro-nano topography increase the hydrophilicity [23].

*Porphyromonas gingivalis* is a Gram-negative, and anaerobic bacteria which is the most common pathogen associated peri implant mucositis and peri implantitis after the implant placement. The MN group indicated the antibacterial higher antibacterial activity compare to the MR and MA. Micro-nano topography is considered an effective strategy for preventing bacterial adhesion. Microscale topographical features, which are comparable in size to *Porphyromonas gingivalis*, typically measuring approximately  $1.51 \mu\text{m}$  in length and  $1 \mu\text{m}$  in diameter, facilitate bacterial positioning to maximize contact with the surface. Conversely, surfaces with micro-nano or nanoscale features, which are substantially smaller than bacterial cells, significantly reduce adhesion by limiting the contact area between the bacterial cells and the surface [7]. Moreover, flower-like topographical structures have been reported to exhibit enhanced antibacterial activity [1].

In addition to surface topography, the chemical composition, surface roughness, and wettability are critical factors influencing the antibacterial activity observed within the MN group. Surface roughness affects the contact area available for bacterial adhesion and increased roughness generally provides more opportunities for bacterial attachment. However, the MN surface roughness may counteract this by reducing the effective contact area, thereby limiting bacterial colonization [7]. Furthermore, wettability significantly influences the interaction between the bacterial membrane and the surface. *Porphyromonas gingivalis*

possesses a hydrophobic outer membrane, and a hydrophilic surface can effectively inhibit the attachment of these hydrophobic bacteria [32]. Overall the combination of the acid etching and alkaline heat treatment supported our hypothesis increase the titanium surface properties and enhance antibacterial effectiveness.

Despite the promising surface properties and antibacterial activity of the MN material, its mechanical properties have not been thoroughly investigated. This study did not confirm the material's effectiveness against Gram-positive pathogens nor fully elucidate the mechanisms underlying its antibacterial activity. From a clinical standpoint, the long-term performance including the wear resistance, biocompatibility, and osseointegration of the combined acid-etching and alkali-heat treatment technique should be thoroughly evaluated in the future. We acknowledge the limitations of this study and emphasize the need for additional research to comprehensively assess the material's mechanical performance, antibacterial mechanisms, and osseointegration potential to gain a more complete understanding of its capabilities and applications.

## CONCLUSION

In conclusion, the combination of acid etching and alkaline heat treatment has shown the ability to create a micro-nano surface with outstanding properties and significant antibacterial effects. This surface modification offers a promising alternative for enhancing the titanium surfaces of dental implants, potentially improving both biological performance and resistance to bacterial adhesion. However, further research is necessary to fully investigate its mechanical properties and long-term effectiveness in clinical applications.

## Acknowledgements

The authors would like to express their sincere gratitude to Tahta Amrillah. for their invaluable assistance in preparing the titanium surface and conducting the XRD analysis.

## Author's Contributions

NK: Conceptualization, Methodology, Validation, Formal Analysis, Investigation, Writing – Original Draft Preparation, Writing – Review & Editing, Visualization, Supervision, and Funding

Acquisition. RMS: Conceptualization, Methodology, Validation, Formal Analysis, Investigation, Writing – Review & Editing, Visualization, Supervision, and Funding Acquisition. KM: Investigation, Writing – Review & Editing, Visualization. SEA: Investigation, Formal Analysis, Writing – Review & Editing, Visualization. ARPG: Investigation, Formal analysis, Writing – Review & Editing. HL: Investigation, Formal analysis, Writing – Review & Editing.

## Conflict of Interest

The authors have no conflicts of interest to declare.

## Funding

This study was supported by a grant from Airlangga Research Fund, Universitas Airlangga, Indonesia, with grant number 267/UN3/2024.

## Regulatory Statement

This study was conducted accordance with ethical guidance and approved by Health Research Ethical Clearance Commission, Faculty of Dental Medicine, Universitas Airlangga, Number 0524/HRECC.FODM/V/2024.

## REFERENCES

- Ding Y, Yuan Z, Hu JW, Xu K, Wang H, Liu P, et al. Surface modification of titanium implants with micro-nano-topography and NIR photothermal property for treating bacterial infection and promoting osseointegration. *Rare Met.* 2022;41(2):673-88. <http://doi.org/10.1007/s12598-021-01830-0>.
- Hou C, An J, Zhao D, Ma X, Zhang W, Zhao W, et al. Surface modification techniques to produce micro/nano-scale topographies on ti-based implant surfaces for improved osseointegration. *Front Bioeng Biotechnol.* 2022;10(3):835008. <http://doi.org/10.3389/fbioe.2022.835008>. PMID:35402405.
- Araujo JCR, Espirito Santo LL, Schneider SG. Influence of titanium nanotubular surfaces, produced by anodization, on the behavior of osteogenic cells: in vitro evaluation. *Braz Dent Sci.* 2022;25(1):1-9. <http://doi.org/10.4322/bds.2022.e2528>.
- Al-Khafaji AM, Issa MI, Ismael FJ, Hamad TI, Aljudy HJ. Poly ether keton keton polymer deposition on laser surface structured commercial pure titanium using magnetron sputtering. *Braz Dent Sci.* 2024;27(2):1-12. <http://doi.org/10.4322/bds.2024.e4234>.
- Banu Raza F, Vijayaragavalu S, Kandasamy R, Krishnaswami V, Kumar VA. Microbiome and the inflammatory pathway in peri-implant health and disease with an updated review on treatment strategies. *J Oral Biol Craniofac Res.* 2023;13(2):84-91. <http://doi.org/10.1016/j.jobcr.2022.11.005>. PMID:36504486.
- Manivasagam VK, Perumal G, Arora HS, Popat KC. Enhanced antibacterial properties on superhydrophobic micro-nano structured titanium surface. *J Biomed Mater Res A.*

- 2022;110(7):1314-28. <http://doi.org/10.1002/jbm.a.37375>. PMID:35188338.
7. Zhai S, Tian Y, Shi X, Liu Y, You J, Yang Z, et al. Overview of strategies to improve the antibacterial property of dental implants. *Front Bioeng Biotechnol.* 2023;11(9):1267128. <http://doi.org/10.3389/fbioe.2023.1267128>. PMID:37829564.
  8. Zheng TX, Li W, Gu YY, Zhao D, Qi MC. Classification and research progress of implant surface antimicrobial techniques. *J Dent Sci.* 2022;17(1):1-7. <http://doi.org/10.1016/j.jds.2021.08.019>. PMID:35028014.
  9. Fernandes VVB Jr, da Rosa PAA, Grisante LAD, Embacher FC, Lopes BB, de Vasconcellos LGO, et al. Argon plasma application on the surface of titanium implants: osseointegration study. *Braz Dent Sci.* 2023;26(4):1-9. <http://doi.org/10.4322/bds.2023.e3843>.
  10. Costa PM Fo, Marcantonio CC, de Oliveira DP, Lopes MES, Puetate JCS, Faria LV, et al. Titanium micro-nano textured surface with strontium incorporation improves osseointegration: an in vivo and in vitro study. *J Appl Oral Sci.* 2024;32:e20240144. <http://doi.org/10.1590/1678-7757-2024-0144>. PMID:39292113.
  11. Tokmedash AM, Kim C, Chavda AP, Li A, Robins J, Min J. Engineering multifunctional surface topography to regulate multiple biological responses. *Biomaterials.* 2025;319(9):123136. <http://doi.org/10.1016/j.biomaterials.2025.123136>. PMID:39978049.
  12. Guo Z, Liu H, Wang W, Hu Z, Li X, Chen H, et al. Recent advances in antibacterial strategies based on TiO<sub>2</sub> biomimetic micro/nano-structured surfaces fabricated using the hydrothermal method. *Biomimetics (Basel).* 2024;9(11):656. <http://doi.org/10.3390/biomimetics9110656>. PMID:39590228.
  13. Kartikasari N, Yamada M, Watanabe J, Tiskratok W, He X, Egusa H. Titania nanospikes activate macrophage phagocytosis by ligand-independent contact stimulation. *Sci Rep.* 2022;12(1):12250. <http://doi.org/10.1038/s41598-022-16214-2>. PMID:35851278.
  14. Yamada M, Kimura T, Nakamura N, Watanabe J, Kartikasari N, He X, et al. Titanium nanosurface with a biomimetic physical microenvironment to induce endogenous regeneration of the periodontium. *ACS Appl Mater Interfaces.* 2022;14(24):27703-19. <http://doi.org/10.1021/acsmi.2c06679>. PMID:35695310.
  15. Kartikasari N, Yamada M, Watanabe J, Tiskratok W, He X, Kamano Y, et al. Titanium surface with nanospikes tunes macrophage polarization to produce inhibitory factors for osteoclastogenesis through nanotopographic cues. *Acta Biomater.* 2022;137:316-30. <http://doi.org/10.1016/j.actbio.2021.10.019>. PMID:34673230.
  16. Kato E, Yamada M, Kokubu E, Egusa H, Ishihara K. Anisotropic patterns of nanospikes induces anti-biofouling and mechano-bactericidal effects of titanium nanosurfaces with electrical cue. *Mater Today Bio.* 2024;29(8):101352. <http://doi.org/10.1016/j.mtbio.2024.101352>. PMID:39669800.
  17. Tan L, Fu J, Feng F, Liu X, Cui Z, Li B, et al. Engineered probiotics biofilm enhances osseointegration via immunoregulation and anti-infection. *Sci Adv.* 2020;6(46):1-10. <http://doi.org/10.1126/sciadv.aba5723>. PMID:33188012.
  18. Martinez Y, Ausina V, Llana C, Montiel JM. Scientific evidence on the efficacy of effervescent tablets for cleaning removable prostheses. A systematic review and meta-analysis. *J Prosthet Dent.* 2024;131(6):1071-83. <http://doi.org/10.1016/j.prosdent.2023.01.031>. PMID:36870893.
  19. Su Y, Komasa S, Sekino T, Nishizaki H, Okazaki J. Nanostructured Ti6Al4V alloy fabricated using modified alkali-heat treatment: characterization and cell adhesion. *Mater Sci Eng C.* 2016;59:617-23. <http://doi.org/10.1016/j.msec.2015.10.077>. PMID:26652415.
  20. Yamada M, Kato E, Yamamoto A, Sakurai K. A titanium surface with nano-ordered spikes and pores enhances human dermal fibroblastic extracellular matrix production and integration of collagen fibers. *Biomed Mater.* 2016;11(1):015010. <http://doi.org/10.1088/1748-6041/11/1/015010>. PMID:26835848.
  21. Jaggessar A, Shahali H, Mathew A, Yarlaga PKDV. Biomimicking nano and micro-structured surface fabrication for antibacterial properties in medical implants. *J Nanobiotechnology.* 2017;15(1):64. <http://doi.org/10.1186/s12951-017-0306-1>. PMID:28969628.
  22. Gao Q, Hou Y, Li Z, Hu J, Huo D, Zheng H, et al. mTORC2 regulates hierarchical micro/nano topography-induced osteogenic differentiation via promoting cell adhesion and cytoskeletal polymerization. *J Cell Mol Med.* 2021;25(14):6695-708. <http://doi.org/10.1111/jcmm.16672>. PMID:34114337.
  23. Chen C, Feng P, Feng F, Zheng Z, Wang J. Micro/nano-surface modification of titanium implant enhancing wear resistance and biocompatibility. *Int J Mech Sci.* 2024;276(May):109385. <http://doi.org/10.1016/j.ijmecsci.2024.109385>.
  24. Nakamura K, Shirato M, Kanno T, Örtengren U, Lingström P, Niwano Y. Antimicrobial activity of hydroxyl radicals generated by hydrogen peroxide photolysis against *Streptococcus mutans* biofilm. *Int J Antimicrob Agents.* 2016;48(4):373-80. <http://doi.org/10.1016/j.ijantimicag.2016.06.007>. PMID:27449541.
  25. Younis AB, Milosavljevic V, Fialova T, Smerkova K, Michalkova H, Svec P, et al. Synthesis and characterization of TiO<sub>2</sub> nanoparticles combined with geraniol and their synergistic antibacterial activity. *BMC Microbiol.* 2023;23(1):207. <http://doi.org/10.1186/s12866-023-02955-1>. PMID:37528354.
  26. Haghi M, Hekmatafshar M, Janipour MB, Gholizadeh SS, Faraz MK, Sayyadifar F, et al. Antibacterial effect of TiO<sub>2</sub> nanoparticles on pathogenic strain of *E. coli*. *Int J Adv Biotechnol Res.* 2012;3(3):621-4.
  27. Serov DA, Gritsaeva AV, Yanbaev FM, Simakin AV, Gudkov SV. Review of antimicrobial properties of titanium dioxide nanoparticles. *Int J Mol Sci.* 2024;25(19):10519. <http://doi.org/10.3390/ijms251910519>. PMID:39408848.
  28. Almalki AH, Hassan WH, Belal A, Farghali A, Saleh RM, Allah AE, et al. Exploring the antimicrobial activity of sodium titanate nanotube biomaterials in combating bone infections: an in vitro and in vivo Study. *Antibiotics (Basel).* 2023;12(5):799. <http://doi.org/10.3390/antibiotics12050799>. PMID:37237702.
  29. Tuikampee S, Chaijareenont P, Rungsiyakull P, Yavirach A. Titanium surface modification techniques to enhance osteoblasts and bone formation for dental implants: a narrative review on current advances. *Metals (Basel).* 2024;14(5):1-28. <http://doi.org/10.3390/met14050515>.
  30. Kato E, Sakurai K, Yamada M. Periodontal-like gingival connective tissue attachment on titanium surface with nano-ordered spikes and pores created by alkali-heat treatment. *Dent Mater.* 2015;31(5):e116-30. <http://doi.org/10.1016/j.dental.2015.01.014>. PMID:25698416.
  31. Joshi B, Regmi C, Dhakal D, Gyawali G, Lee SW. Efficient inactivation of *Staphylococcus aureus* by silver and copper loaded photocatalytic titanate nanotubes. *Prog Nat Sci.* 2018;28(1):15-23. <http://doi.org/10.1016/j.pnsc.2018.01.004>.
  32. Liu J, Liu J, Attarilar S, Wang C, Tamaddon M, Yang C, et al. Nano-modified titanium implant materials: a way toward improved antibacterial properties. *Front Bioeng Biotechnol.* 2020;8(11):576969. <http://doi.org/10.3389/fbioe.2020.576969>. PMID:33330415.
  33. Ziegelmeier T, Martins de Sousa K, Liao TY, Lartizien R, Delay A, Vollaire J, et al. Multifunctional micro/nano-textured titanium with bactericidal, osteogenic, angiogenic and anti-inflammatory properties: insights from in vitro and in vivo studies. *Mater Today Bio.* 2025;32(12):101710. <http://doi.org/10.1016/j.mtbio.2025.101710>. PMID:40230651.
  34. Papa S, Maalouf M, Claudel P, Sedao X, Di Maio Y, Hamzeh-Cognasse H, et al. Key topographic parameters driving surface adhesion of *Porphyromonas gingivalis*. *Sci Rep.* 2023;13(1):15893. <http://doi.org/10.1038/s41598-023-42387-5>. PMID:37741851.

**Nadia Kartikasari**

**(Corresponding address)**

Universitas Airlangga, Department of Prosthodontic, Faculty of Dental Medicine,  
Surabaya, Jawa Timur, Indonesia.

Email: nadiakartikasari@fkg.unair.ac.id

Date submitted: 2025 Jan 23

Accept submission: 2025 Apr 22